Vol 458|30 April 2009|doi:10.1038/nature08017

LETTERS

Greenhouse-gas emission targets for limiting global warming to 2 °C

Malte Meinshausen[1], Nicolai Meinshausen[2], William Hare[1,3], Sarah C. B. Raper[4], Katja Frieler[1], Reto Knutti[5], David J. Frame[6,7] & Myles R. Allen[7]

More than 100 countries have adopted a global warming limit of 2 °C or below (relative to pre-industrial levels) as a guiding principle for mitigation efforts to reduce climate change risks, impacts and damages[1,2]. However, the greenhouse gas (GHG) emissions corresponding to a specified maximum warming are poorly known owing to uncertainties in the carbon cycle and the climate response. Here we provide a comprehensive probabilistic analysis aimed at quantifying GHG emission budgets for the 2000–50 period that would limit warming throughout the twenty-first century to below 2 °C, based on a combination of published distributions of climate system properties and observational constraints. We show that, for the chosen class of emission scenarios, both cumulative emissions up to 2050 and emission levels in 2050 are robust indicators of the probability that twenty-first century warming will not exceed 2 °C relative to pre-industrial temperatures. Limiting cumulative CO_2 emissions over 2000–50 to 1,000 Gt CO_2 yields a 25% probability of warming exceeding 2 °C—and a limit of 1,440 Gt CO_2 yields a 50% probability—given a representative estimate of the distribution of climate system properties. As known 2000–06 CO_2 emissions[3] were ~234 Gt CO_2, less than half the proven economically recoverable oil, gas and coal reserves[4–6] can still be emitted up to 2050 to achieve such a goal. Recent G8 Communiqués[7] envisage halved global GHG emissions by 2050, for which we estimate a 12–45% probability of exceeding 2 °C—assuming 1990 as emission base year and a range of published climate sensitivity distributions. Emissions levels in 2020 are a less robust indicator, but for the scenarios considered, the probability of exceeding 2 °C rises to 53–87% if global GHG emissions are still more than 25% above 2000 levels in 2020.

Determining probabilistic climate change for future emission scenarios is challenging, as it requires a synthesis of uncertainties along the cause–effect chain from emissions to temperatures; for example, uncertainties in the carbon cycle[8], radiative forcing and climate responses. Uncertainties in future climate projections can be quantified by constraining climate model parameters to reproduce historical observations of temperature[9], ocean heat uptake[10] and independent estimates of radiative forcing. By focusing on emission budgets (the cumulative emissions to stay below a certain warming level) and their probabilistic implications for the climate, we build on pioneering mitigation studies[11,12]. Previous probabilistic studies—while sometimes based on more complex models—either considered uncertainties only in a few forcing components[13], applied relatively simple likelihood estimators ignoring the correlation structure of the observational errors[14] or constrained only model parameters like climate sensitivity rather than allowed emissions.

Using a reduced complexity coupled carbon cycle–climate model[15,16], we constrain future climate projections, building on the Fourth IPCC Assessment Report (AR4) and more recent research. In particular, multiple uncertainties in the historical temperature observations[9] are treated separately for the first time; new ocean heat uptake estimates are incorporated[10]; a constraint on changes in effective climate sensitivity is introduced; and the most recent radiative forcing uncertainty estimates for individual forcing agents are considered[17].

The data constraints provide us with likelihood estimates for the chosen 82-dimensional space of climate response, gas-cycle and radiative forcing parameters (Supplementary Fig. 3). We chose a Bayesian approach, but also obtain 'frequentist' confidence intervals for climate sensitivity (68% interval, 2.3–4.5 °C; 90%, 2.1–7.1 °C), which is in approximate agreement with the recent AR4 estimates. Given the inherent subjectivity of Bayesian priors, we chose priors for climate sensitivity such that we obtain marginal posteriors identical to 19 published climate sensitivity distributions (Fig. 1a). These distributions are not all independent and not equally likely, and cannot be formally combined[18]. They are used here simply to represent the wide variety of modelling approaches, observational data and likelihood derivations used in previous studies, whose implications for an emission budget have not been analysed before. For illustrative purposes, we chose the climate sensitivity distribution of ref. 19 with a uniform prior in transient climate response (TCR, defined as the global-mean temperature change which occurs at the time of CO_2 doubling for the specific case of a 1% yr^{-1} increase of CO_2) as our default. This distribution closely resembles the AR4 estimate (best estimate, 3 °C; likely range, 2.0–4.5 °C) (Supplementary Information).

Maximal warming under low emission scenarios is more closely related to the TCR than to the climate sensitivity[19]. The distribution of the TCR of our climate model for the illustrative default is slightly lower than derived within another model set-up[19], but within the range of results of previous studies (Fig. 1b), and encompasses the range arising from emulations by coupled atmosphere–ocean general circulation models[16] (AOGCMs) (Fig. 1c).

Representing current knowledge on future carbon-cycle responses is difficult, and might be best encapsulated in the wide range of results from the process-based C4MIP carbon-cycle models[8]. We emulate these C4MIP models individually by calibrating 18 parameters in our carbon-cycle model[16], and combine these settings with the other gas cycles, radiative forcing and climate response parameter uncertainties gained from our historical constraining.

Additional challenges arise in estimating the maximum temperature change resulting from a certain amount of cumulative emissions. The analysis needs to be based on a multitude of emission pathways with realistic multi-gas characteristics[20,21], as well as varying

[1]Potsdam Institute for Climate Impact Research, Telegraphenberg, 14412 Potsdam, Germany. [2]Department of Statistics, University of Oxford, South Parks Road, Oxford OX1 3TG, UK. [3]Climate Analytics, Telegraphenberg, 14412 Potsdam, Germany. [4]Centre for Air Transport and the Environment, Manchester Metropolitan University, Chester Street, Manchester M1 5GD, UK. [5]Institute for Atmospheric and Climate Science, ETH Zurich, 8092 Zurich, Switzerland. [6]Smith School of Enterprise and the Environment, University of Oxford, Oxford OX1 2BQ, UK. [7]Department of Physics, University of Oxford, Parks Road, Oxford OX1 3PU, UK.

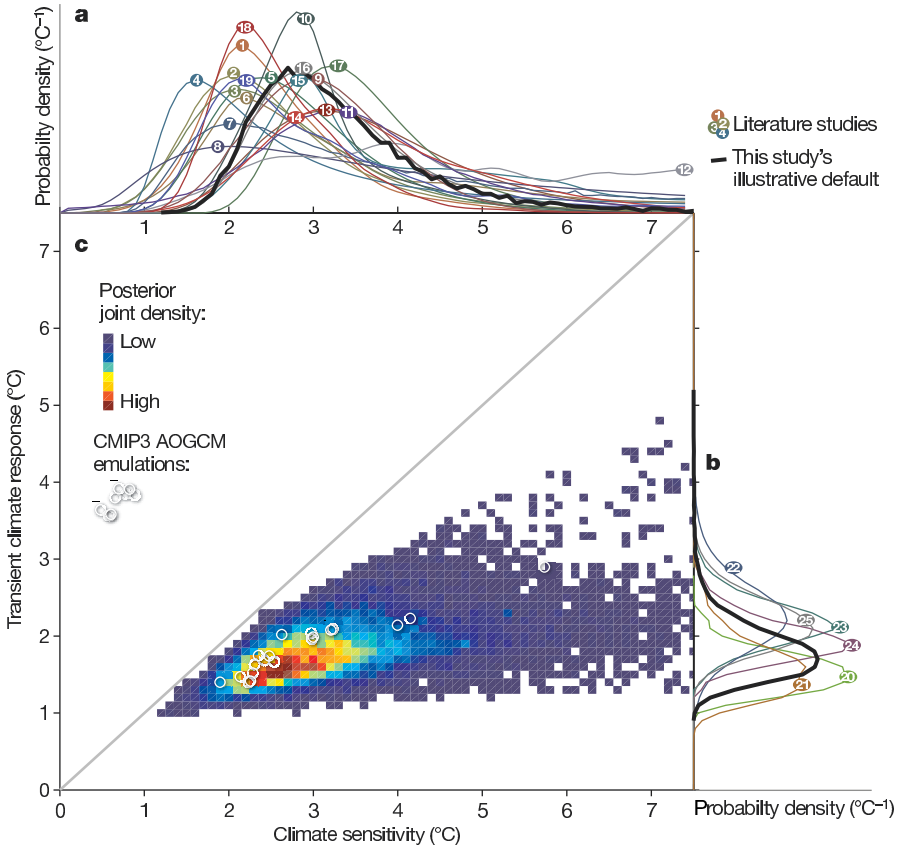

Figure 1 | Joint and marginal probability distributions of climate sensitivity and transient climate response. **a**, Marginal probability density functions (PDFs) of climate sensitivity; **b**, marginal PDFs of transient climate response (TCR); **c**, posterior joint distribution constraining model parameters to historical temperatures, ocean heat uptake and radiative forcing under our representative illustrative priors. For comparison, TCR and climate sensitivities are shown in **c** for model versions that yield a close emulation of 19 CMIP3 AOGCMs (white circles)[16]. Data sources for curves 1–25 are given in Supplementary Information.

shapes over time. AOGCM results for multi-gas mitigation scenarios were not available for assessment in the IPCC AR4 Working Group I Report[22]. Consequently, IPCC AR4 Working Group III[23] provided equilibrium warming estimates corresponding to 2100 radiative forcing levels for some multi-gas mitigation scenarios, using simplified regressions (Supplementary Fig. 6). Thus, 15 years after the first pioneering mitigation studies[11,12], there is still an important gap in the literature relating emission budgets for lower emission profiles to the probability of exceeding maximal warming levels; a gap that this study intends to fill.

We compute time-evolving distributions of radiative forcing and surface air temperature implications for the set of 26 IPCC SRES[21] and 20 EMF-21 scenarios[20] shown in Fig. 2a and b. We complement these with 948 multi-gas equal quantile walk emission pathways[24] that share—by design—similar multi-gas characteristics (Supplementary Fig. 5) but represent a wide variety of plausible shapes, ranging from early moderate reductions to later peaking and rapidly declining emissions towards near-zero emissions (Supplementary Information). Whereas Fig. 2e shows a standard plot of global-mean temperature versus time for two sample scenarios, Fig. 2f highlights the strong correlation between maximum warming and cumulative emissions. The fraction of climate model runs above 2 °C (dashed line in Fig. 2f) is then our estimate for the probability of exceeding 2 °C for an individual scenario (as indicated by the dots in Fig. 3a). We focus here on 2 °C relative to pre-industrial levels, as such a warming limit has gained increasing prominence in science and policy circles as a goal to prevent dangerous climate change[25]. We recognize that 2 °C cannot be regarded as a 'safe level', and that (for example) small island states and least developed countries are calling for warming to be limited to 1.5 °C (Supplementary Information). We chose the twenty-first century as our time horizon, as this time frame is sufficiently long to determine which emission scenarios will probably lead to a global surface warming below 2 °C. Under these scenarios, temperatures have stabilized or peaked by 2100, while warming continues under higher scenarios.

For our illustrative distribution of climate system properties, we find that the probability of exceeding 2 °C can be limited to below 25% (50%) by keeping 2000–49 cumulative CO_2 emissions from fossil sources and land use change to below 1,000 (1,440) Gt CO_2 (Fig. 3a and Table 1). If we resample model parameters to reproduce 18 published climate sensitivity distributions, we find a 10–42% probability of exceeding 2 °C for such a budget of 1,000 Gt CO_2. If the acceptable exceedance probability were only 20%, this would require an emission budget of 890 Gt CO_2 or lower (illustrative default). Given that around 234 Gt CO_2 were emitted between 2000 and 2006 and assuming constant rates of 36.3 Gt CO_2 yr^{-1} (ref. 3) thereafter, we would exhaust the CO_2 emission budget by 2024, 2027 or 2039, depending on the probability accepted for exceeding 2 °C (respectively 20%, 25% or 50%).

To contrast observationally constrained probabilistic projections against current AOGCM and carbon-cycle models, we ran each emission scenario with all permutations of 19 CMIP3[26] AOGCM and 10 C4MIP carbon-cycle model emulations[16]. The allowed emissions are similar to the lower part of the range spanned by the observationally constrained distributions, suggesting that the current AOGCMs do not substantially over- or underestimate future climate change compared to the values obtained using a model constrained by observations, although no probability statement can be derived from the proportion of runs exceeding 2 °C (black dashed line in Fig. 3a). Using an independent approach focusing on CO_2 alone, Allen *et al.*[27]

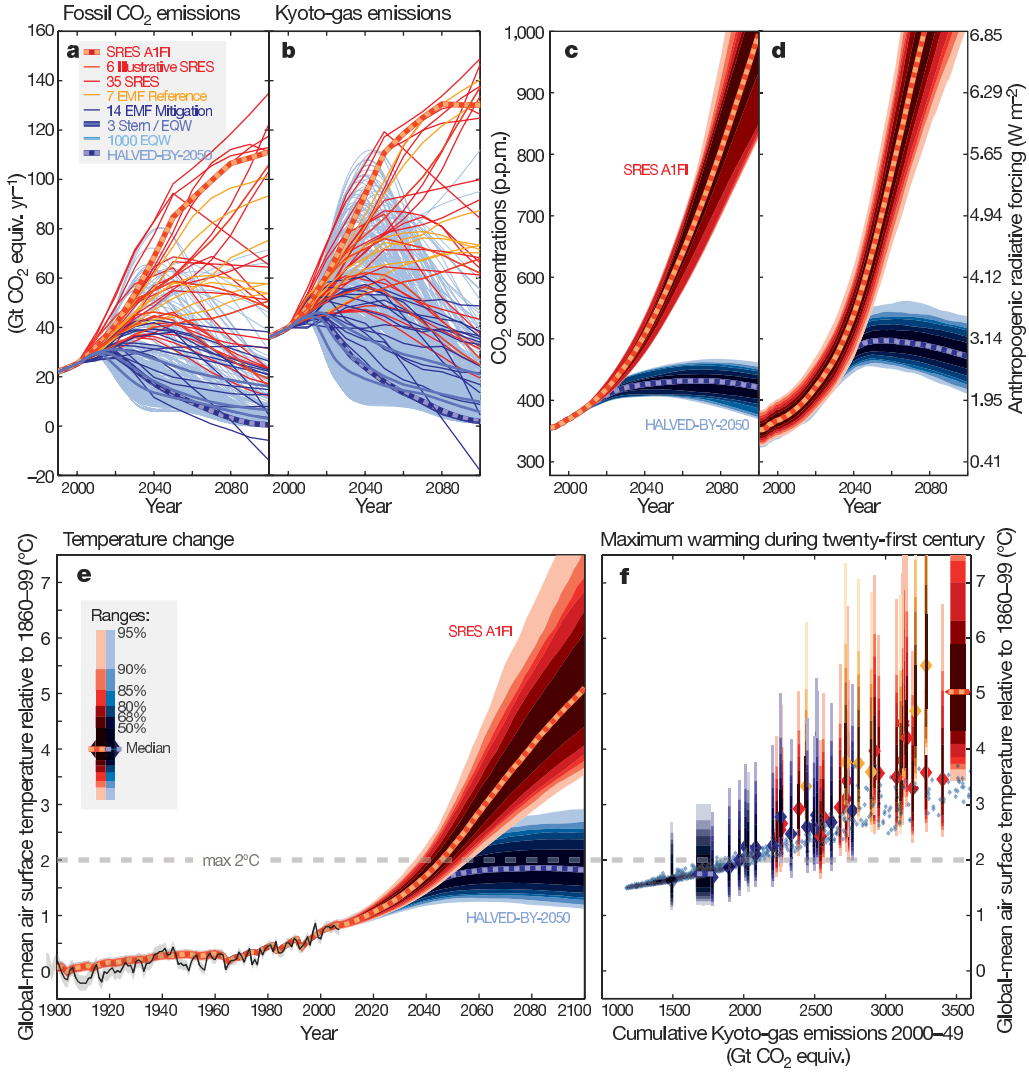

Figure 2 | Emissions, concentrations and twenty-first century global-mean temperatures. a, Fossil CO_2 emissions for IPCC SRES[21], EMF-21[20] scenarios and a selection of equal quantile walk[24] (EQW) pathways analysed here; **b,** GHGs, as controlled under the Kyoto Protocol; **c,** median projections and uncertainties based on our illustrative default case for atmospheric CO_2 concentrations for the high SRES A1FI[21] and the low HALVED-BY-2050[30] scenario, which halves 1990 global Kyoto-gas emissions by 2050; **d,** total anthropogenic radiative forcing; **e,** surface air global-mean temperature; **f,** maximum temperature during the twenty-first century versus cumulative Kyoto-gas emissions for 2000–49. Colour range shown in **e** also applies to **c, d** and **f.**

find that a range of 2,050–2,100 Gt CO_2 emissions from year 2000 onwards cause a most likely CO_2-induced warming of 2 °C: in the idealized scenarios they consider that meet this criterion, between 1,550 and 1,950 Gt CO_2 are emitted over the years 2000 to 2049.

We explored the consequences of burning all proven fossil fuel reserves (the fraction of fossil fuel resources that is economically recoverable with current technologies and prices: Fig. 3b and Methods). We derived a mid-estimate of 2,800 Gt CO_2 emissions from the literature, with an 80%-uncertainty range of 2,541 to 3,089 Gt CO_2. Emitting the carbon from all proven fossil fuel reserves would therefore vastly exceed the allowable CO_2 emission budget for staying below 2 °C.

Although the dominant anthropogenic warming contribution is from CO_2 emissions, non-CO_2 GHG emissions add to the risk of exceeding warming thresholds during the twenty-first century. We estimate that the so-called non-CO_2 'Kyoto gases' (methane, nitrous oxide, hydrofluorocarbons, perfluorocarbons and SF_6) will constitute roughly one-third of total CO_2 equivalent (CO_2 equiv.) emissions based on 100-yr global warming potentials[28] over the 2000–49 period. Under our illustrative distribution for climate system properties, and taking into account all positive and negative forcing agents as provided by Table 2.12 in AR4[17], the cumulative Kyoto-gas emission budget for 2000–50 is 1,500 (2,000) Gt CO_2 equiv., if the probability of exceeding 2 °C is to be limited to approximately 25% (50%) (Table 1).

For the lower scenarios, Kyoto-gas emissions in the year 2050 are a remarkably good indicator for probabilities of exceeding 2 °C, because for these scenarios (with emissions in 2050 below ~30 Gt CO_2 equiv.), radiative forcing peaks around 2050 and temperature soon thereafter. This is indicated by the narrow spread of individual scenarios' exceedance probabilities for similar 2050 Kyoto-gas emissions, as shown in Supplementary Fig. 1b. If emissions in 2050 are half 1990 levels, we estimate a 12–45% probability of exceeding 2 °C (Table 1) under these scenarios.

Emissions in 2020 are a less robust indicator of maximum warming (note the wide vertical spread of individual scenario dots in Supplementary Fig. 1c)—even if restricted to this class of relatively smooth emission pathways. However, the probability of exceeding 2 °C rises to 75% if 2020 emissions are not lower than 50 Gt CO_2 equiv. (25% above 2000). Given the substantial recent increase in fossil CO_2 emissions (20% between 2000 and 2006)[3], policies to reduce global emissions are needed urgently if the 'below 2 °C' target[29] is to remain achievable.

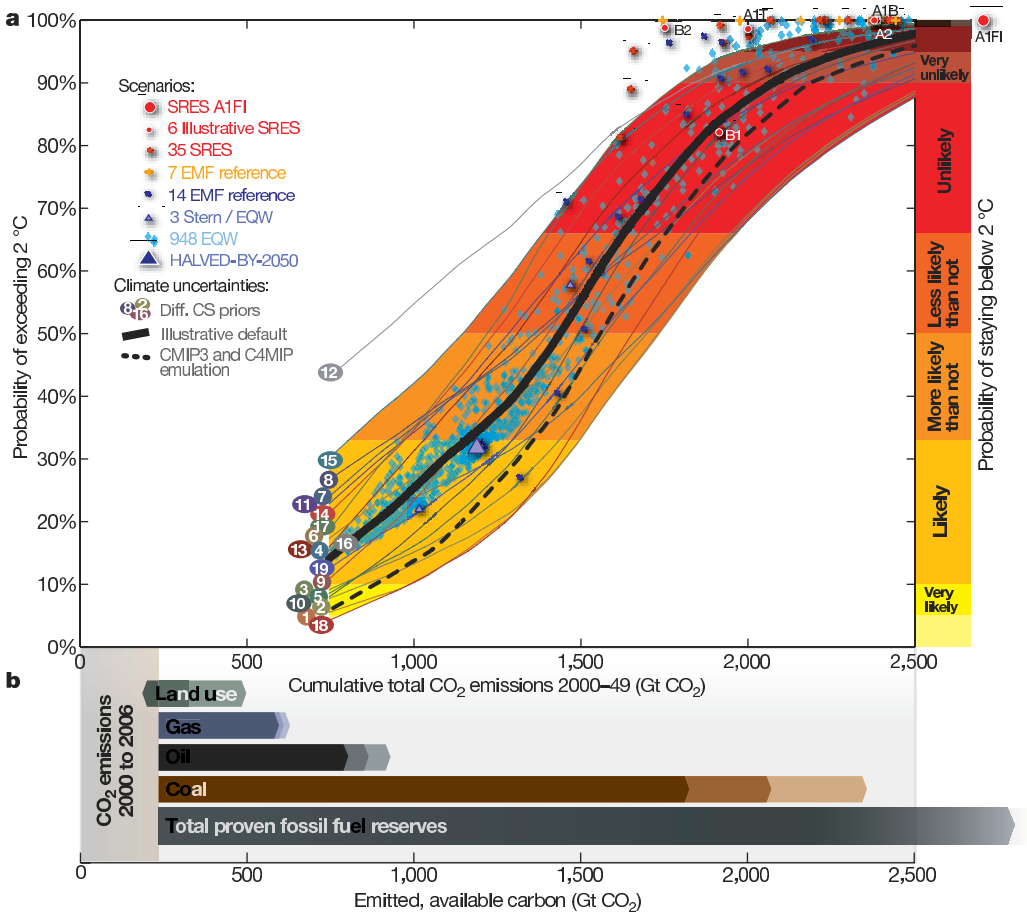

Figure 3 | The probability of exceeding 2 °C warming versus CO_2 emitted in the first half of the twenty-first century. a, Individual scenarios' probabilities of exceeding 2 °C for our illustrative default (dots; for example, for SRES B1, A2, Stern and other scenarios shown in Fig. 2) and smoothed (local linear regression smoother) probabilities for all climate sensitivity distributions (numbered lines, see Supplementary Information for data sources). The proportion of CMIP3 AOGCMs[26] and C4MIP carbon-cycle[8] model emulations exceeding 2 °C is shown as black dashed line. Coloured areas denote the range of probabilities (right) of staying below 2 °C in AR4 terminology, with the extreme upper distribution (12) being omitted. **b,** Total CO_2 emissions already emitted[3] between 2000 and 2006 (grey area) and those that could arise from burning available fossil fuel reserves, and from land use activities between 2006 and 2049 (median and 80% ranges, Methods).

Table 1 | Probabilities of exceeding 2 °C

Indicator	Emissions	Probability of exceeding 2 °C*	
		Range	Illustrative default case‡
Cumulative total CO_2 emission 2000–49	886 Gt CO_2	8–37%	20%
	1,000 Gt CO_2	10–42%	25%
	1,158 Gt CO_2	16–51%	33%
	1,437 Gt CO_2	29–70%	50%
Cumulative Kyoto-gas emissions 2000–49	1,356 Gt CO_2 equiv.	8–37%	20%
	1,500 Gt CO_2 equiv.	10–43%	26%
	1,678 Gt CO_2 equiv.	15–51%	33%
	2,000 Gt CO_2 equiv.	29–70%	50%
2050 Kyoto-gas emissions	10 Gt CO_2 equiv. yr^{-1}	6–32%	16%
	(Halved 1990) 18 Gt CO_2 equiv. yr^{-1}	12–45%	29%
	(Halved 2000) 20 Gt CO_2 equiv. yr^{-1}	15–49%	32%
	36 Gt CO_2 equiv. yr^{-1}	39–82%	64%
2020 Kyoto-gas emissions	30 Gt CO_2 equiv. yr^{-1}	(8–38%)†	(21%)†
	35 Gt CO_2 equiv. yr^{-1}	(13–46%)†	(29%)†
	40 Gt CO_2 equiv. yr^{-1}	(19–56%)†	(37%)†
	50 Gt CO_2 equiv. yr^{-1}	(53–87%)†	(74%)†

* Range across all priors reflecting the various climate sensitivity distributions with the exception of line 12 in Fig. 3a.
† Note that 2020 Kyoto-gas emissions are, from a physical perspective, a less robust indicator for maximal twenty-first century warming with a wide scenario-to-scenario spread (Supplementary Fig. 1c).
‡ Prior chosen to match posterior of ref. 19 with uniform priors on the TCR.

METHODS SUMMARY

To relate emissions of GHGs, tropospheric ozone precursors and aerosols to gas-cycle and climate system responses, we employ MAGICC 6.0[16], a reduced complexity coupled climate–carbon cycle model used in past IPCC assessment reports for emulating AOGCMs. Out of more than 400 parameters, we vary 9 climate response parameters (one of which is climate sensitivity), 33 gas-cycle and global radiative forcing parameters (not including 18 carbon-cycle parameters, which are calibrated separately[16] to C4MIP carbon-cycle models[8]), and 40 scaling factors determining the regional 4 box pattern of key forcings (Supplementary Table 1). Other parameters are set to default values[16].

To constrain the parameters, we use observational data of surface air temperature[9] in 4 spatial grid boxes from 1850 to 2006, the linear trend in ocean heat content changes[10] from 1961 to 2003 and year 2005 radiative forcing estimates

for 18 forcing agents[17], in addition to a constraint on the twenty-first century change of effective climate sensitivity derived from AOGCM CMIP3 emulations[16]. With a Metropolis-Hastings Markov chain Monte Carlo approach, based on a large ensemble ($>3\times10^6$) of parameter sets using 45 parallel Markov chains with 75,000 runs each, we estimate the posterior distribution of different MAGICC parameters. Estimated likelihoods take into account observational uncertainty and climate variability from various AOGCM control runs, HadCM3 being the default.

For forward projections with the model, we combine, at random, 600 sets of the 82 historically constrained parameters with one of 10 carbon-cycle calibrations. We supplemented 26 multi-gas IPCC SRES[21] and 20 EMF-21 reference and mitigation scenarios[20] by 948 equal quantile walk multi-gas pathways[24]. The proven fossil fuel reserve estimates for natural gas, oil and coal were compiled from various sources[4,5] by combining the reserve estimates with net calorific values and emission factors (and their 95% uncertainty ranges) according to IPCC 2006 guidelines[6] (Supplementary Information).

Full Methods and any associated references are available in the online version of the paper at www.nature.com/nature.

Received 25 September 2008; accepted 25 March 2009.

1. Pachauri, R. K. & Reisinger, A. (eds) *Climate Change 2007: Synthesis Report* (Intergovernmental Panel on Climate Change, Cambridge, UK, 2007).
2. Council of the European Union. *Presidency Conclusions – Brussels, 22/23 March 2005* (European Commission, 2005).
3. Canadell, J. G. *et al.* Contributions to accelerating atmospheric CO_2 growth from economic activity, carbon intensity, and efficiency of natural sinks. *Proc. Natl Acad. Sci. USA* **104,** 18866–18870 (2007).
4. Clarke, A. W. & Trinnaman, J. A. (eds) *2007 Survey of Energy Resources* (World Energy Council, 2007).
5. Rempe, H. Schmidt, S. & Schwarz-Schampera, U. *Reserves, Resources and Availability of Energy Resources 2006* (German Federal Institute for Geosciences and Natural Resources, 2007).
6. Eggelston, H. S., Buendia, L., Miwa, K., Ngara, T. & Tanabe, K. (eds) *2006 Guidelines for National Greenhouse Gas Inventories* (IPCC National Greenhouse Gas Inventories Programme, Hayama, Japan, 2006).
7. G8. *Hokkaido Toyako Summit Leaders Declaration* (G8, 2008); available at ⟨http://www.mofa.go.jp/policy/economy/summit/2008/doc/doc080714_en.html⟩.
8. Friedlingstein, P. *et al.* Climate–carbon cycle feedback analysis: Results from the C4MIP model intercomparison. *J. Clim.* **19,** 3337–3353 (2006).
9. Brohan, P., Kennedy, J. J., Harris, I., Tett, S. F. B. & Jones, P. D. Uncertainty estimates in regional and global observed temperature changes: A new data set from 1850. *J. Geophys. Res.* **111,** D12106, doi:10.1029/2005JD006548 (2006).
10. Domingues, C. M. *et al.* Improved estimates of upper-ocean warming and multi-decadal sea-level rise. *Nature* **453,** 1090–1093 (2008).
11. Enting, I. G., Wigley, T. M. L. & Heimann, M. *Future Emissions and Concentrations of Carbon Dioxide: Key Ocean/Atmosphere/Land Analyses* (Research technical paper no. 31, CSIRO Division of Atmospheric Research, 1994).
12. Wigley, T. M. L., Richels, R. & Edmonds, J. A. Economic and environmental choices in the stabilization of atmospheric CO_2 concentrations. *Nature* **379,** 240–243 (1996).
13. Forest, C. E., Stone, P. H., Sokolov, A., Allen, M. R. & Webster, M. D. Quantifying uncertainties in climate system properties with the use of recent climate observations. *Science* **295,** 113–117 (2002).
14. Knutti, R., Stocker, T. F., Joos, F. & Plattner, G. K. Constraints on radiative forcing and future climate change from observations and climate model ensembles. *Nature* **416,** 719–723 (2002).
15. Wigley, T. M. L. & Raper, S. C. B. Interpretation of high projections for global-mean warming. *Science* **293,** 451–454 (2001).
16. Meinshausen, M., Raper, S. C. B. & Wigley, T. M. L. Emulating IPCC AR4 atmosphere-ocean and carbon cycle models for projecting global-mean, hemispheric and land/ocean temperatures: MAGICC 6.0. *Atmos. Chem. Phys. Discuss.* **8,** 6153–6272 (2008).
17. Forster, P. *et al.* in *IPCC Climate Change 2007: The Physical Science Basis* (eds Solomon, S. *et al.*) 129–234 (Cambridge Univ. Press, 2007).
18. Knutti, R. & Hegerl, G. C. The equilibrium sensitivity of the Earth's temperature to radiation changes. *Nature Geosci.* **1,** 735–743 (2008).
19. Frame, D. J., Stone, D. A., Stott, P. A. & Allen, M. R. Alternatives to stabilization scenarios. *Geophys. Res. Lett.* **33,** L14707, doi:10.1029/2006GL025801 (2006).
20. Van Vuuren, D. P. *et al.* Temperature increase of 21st century mitigation scenarios. *Proc. Natl Acad. Sci. USA* **105,** 15258–15262 (2008).
21. Nakicenovic, N. & Swart, R. *IPCC Special Report on Emissions Scenarios* (Cambridge Univ. Press, 2000).
22. Solomon, S. *et al.* (eds) *IPCC Climate Change 2007: The Physical Science Basis* (Cambridge Univ. Press, 2007).
23. Metz, B., Davidson, O. R., Bosch, P. R., Dave, R. & Meyer, L. A. (eds) *IPCC Climate Change 2007: Mitigation* (Cambridge Univ. Press, 2007).
24. Meinshausen, M. *et al.* Multi-gas emission pathways to meet climate targets. *Clim. Change* **75,** 151–194 (2006).
25. Schellnhuber, J. S., Cramer, W., Nakicenovic, N., Wigley, T. M. L. & Yohe, G. *Avoiding Dangerous Climate Change* (Cambridge Univ. Press, 2006).
26. Meehl, G. A., Covey, C., McAvaney, B., Latif, M. & Stouffer, R. J. Overview of coupled model intercomparison project. *Bull. Am. Meteorol. Soc.* **86,** 89–93 (2005).
27. Allen, M. R. *et al.* Warming caused by cumulative carbon emissions towards the trillionth tonne. *Nature* doi:10.1038/nature08019 (this issue).
28. Houghton, J. T. *et al.* (eds) *IPCC Climate Change 1995: The Science of Climate Change* (Cambridge Univ. Press, 1996).
29. den Elzen, M. G. J. & Meinshausen, M. Meeting the EU 2°C climate target: global and regional emission implications. *Clim. Policy* **6,** 545–564 (2006).
30. Watkins, K. *et al. Fighting Climate Change: Human Solidarity in a Divided World* (Human Development Report 2007/2008, Palgrave Macmillan, 2007).

Supplementary Information is linked to the online version of the paper at www.nature.com/nature.

Acknowledgements We thank T. Wigley, M. Schaeffer, K. Briffa, R. Schofield, T. S., von Deimling, J. Nabel, J. Rogelj, V. Huber and A. Fischlin for discussions and comments on earlier manuscripts and our code, J. Gregory for AOGCM diagnostics, D. Giebitz-Rheinbay and B. Kriemann for IT support and the EMF-21 modelling groups for providing their emission scenarios. M.M. thanks DAAD and the German Ministry of Environment for financial support. We acknowledge the modelling groups, the Program for Climate Model Diagnosis and Intercomparison (PCMDI) and the WCRP's Working Group on Coupled Modelling (WGCM) for their roles in making available the WCRP CMIP3 multi-model data set. Support of this data set is provided by the Office of Science, US Department of Energy.

Author Contributions M.M. and N.M. designed the research with input from W.H., R.K. and M.A. M.M. performed the climate modelling, N.M. the statistical analysis, W.H. the compilation of fossil fuel reserve estimates; all authors contributed to writing the paper.

Author Information Reprints and permissions information is available at www.nature.com/reprints. Accompanying datasets are available at www.primap.org. Correspondence and requests for materials should be addressed to M.M. (malte.meinshausen@pik-potsdam.de).

METHODS

Coupled carbon cycle–climate model. We use a reduced complexity coupled carbon cycle climate model (MAGICC 6.0), requiring (hemispheric) emissions of GHGs, aerosols, and tropospheric ozone precursors as inputs for calculating atmospheric concentrations, radiative forcings, surface air temperatures, and ocean heat uptake. MAGICC is able to closely emulate both CMIP3[26] AOGCMs and C4MIP[8] carbon-cycle models, and has been used extensively in past IPCC assessment reports[16]. We use MAGICC 6.0 here both for future climate projections based on historical constraints and for emulating more complex AOGCMs or carbon-cycle models. The model contains many parameters whose values are uncertain. We looked at the impact of 82 parameters on model behaviour, which are summarized in the vector $\mathbf{\Theta}$.

Observational constraints. As one set of observational constraints, we use yearly averaged temperatures in our four grid boxes (Northern and Southern Hemisphere Land and Ocean) as provided in ref. 9 for the years 1850–2006. We arrange those measurements in a 628-dimensional vector $\mathbf{T}$. The respective space-time dependency of the errors is obtained from ref. 9. We use the full-length control runs of all AOGCMs runs available at PCMDI (http://www-pcmdi.llnl.gov/, as of mid-2007) to assess internal variability. We project the 628-dimensional vector of temperature observations into a low-dimensional subspace. We choose m so that 99.95% of the MAGICC variance is preserved and find that an eight-dimensional subspace is sufficient but findings are insensitive to this choice. We then find the $m \times 628$-dimensional matrix P_m, which corresponds to the projection of $\mathbf{T}$ into the space spanned by the first m PCA components. The likelihood is finally based on the m-dimensional vector $\mathbf{T}_m = P_m\mathbf{T}$ instead of the 628-dimensional vector $\mathbf{T}$. We now assume that the internal variability of $\mathbf{T}_m$ has a Gaussian distribution and estimate the $m \times m$-dimensional covariance matrix Σ_m from the data set as $P_m \Sigma {P_m}^T$, where Σ is the previously derived covariance matrix of the observations (including internal variability and measurement errors).

Ocean heat uptake is only considered via its linear trend Z_1 of $+0.3721$ (1σ: ± 0.0698) 10^{22} J yr^{-1} for the heat content trend over 1961 to 2003 up to 700 m depth[10]. See Supplementary Fig. 2 for the match between the constrained model results and the observational data[31] as well as more recent results[10].

Radiative forcing estimates as listed in ref. 17 (Table 2.12 therein) provide an additional set of 17 constraints $Z_2,\ldots,Z_{18}$ (Supplementary Table 2). The error of 14 of these radiative forcing estimates is assumed to have a Gaussian distribution. The remaining 3 observational constraints, however, exhibit skewness, which we model by a distribution we call here 'skewed normal' (Supplementary Information). All radiative forcing uncertainties are assumed to be independent.

Given that MAGICC 6.0 has substantially more freedom to change the effective climate sensitivity over time[16] than what is observed from AOGCM diagnostics, we introduce another constraint Z_{19}. This constraint limits the ratio of the twenty-first century change in effective climate sensitivity, expressed by the ratio of average effective climate sensitivities in the periods 2050–2100 and 1950–2000. Based on AOGCM CMIP3 model emulations[16], we derive a distribution with a median at 1.23 (with a 90% range between 1.06 to 1.51) under the SRES A1B scenario.

Likelihood estimation. To calculate the likelihood, the observations are split into the projected temperature observations $\mathbf{T}_m$ and the remaining observational constraints $Z_1,\ldots,Z_{19}$. Let f be the density of temperature observations under a given parameter setting $\mathbf{\Theta}$, taking into account both the measurement errors and internal climate variability. Let h_k, $k = 1,\ldots,19$, be the density functions of the remaining observational constraints. Under independence of $Z_1,\ldots,Z_{19}$ and $\mathbf{T}$, the likelihood $L(\mathbf{\Theta})$ of model parameters $\mathbf{\Theta}$ is given by:

$$L(\mathbf{\Theta}) = f(T_m|\mathbf{\Theta}) \prod_{k=1}^{19} h_k(Z_k|\mathbf{\Theta})$$

We follow mostly a Bayesian approach. A prior distribution π over the parameter vector $\mathbf{\Theta}$ is specified in various ways as discussed further below, see Supplementary Table 1 for prior assumption on key parameters. Given the a priori assumption, we are able to specify the posterior distribution $g(\mathbf{\Theta})$ of the parameters as proportional to the product of the likelihood $L(\mathbf{\Theta})$ and the prior $\pi(\mathbf{\Theta})$.

Sensitivity to the chosen prior and a comparison with frequentist inference are discussed further below. For frequentist inference, we work directly with the likelihood.

Model sampling. To draw models from the posterior distribution $g(\mathbf{\Theta})$, we use a Markov chain Monte Carlo approach and a standard Metropolis-Hastings algorithm with adaptive step sizes to attain an average acceptance rate of 60%. 45 Markov chains are run in parallel for 75,000 iterations each. Adjusting for a burn-in time of 20,000 iterations, and retaining only every 30th model, to decrease dependence between successive models, a total of 82,500 models are drawn from the posterior distribution. For probabilistic forecasts, 600 models with maximal spacing in this set of 82,500 models are retained and combined randomly with one of the 10 parameter sets used for emulating individual C4MIP carbon-cycle models[16].

Representation of climate sensitivity distributions. Apart from the frequentist likelihood confidence intervals, we represent the wide range of literature studies on Bayesian climate sensitivity distributions[19,32–41]. Specifically, we change the prior for climate sensitivity such that a match between our posterior PDF of climate sensitivity and the posterior distribution in the considered studies is achieved.

Fossil fuel reserves. Our median estimates of proven recoverable fossil fuel reserves are based on ref. 42, with the exception of the non-conventional oil reserves which are taken as the median between ref. 43 and ref. 44. Potential emissions are estimated using IPCC 2006 default net calorific values and carbon content emission factors[6] (Table 1.2 and Table 1.3 therein).

We estimate the 80% uncertainty range in these reserve estimates as being $\pm 10\%$ of the WEC[42] estimates or the range of estimates in the literature[4,43–46], whichever is greater, for individual classes of reserves. We combine these reserve uncertainties with the provided 95% ranges of calorific values and emission factors for each class of energy reserves[6] (Supplementary Table 3). See Supplementary Information for an expanded description of the methods.

31. Levitus, S., Antonov, J. & Boyer, T. Warming of the world ocean, 1955-2003. *Geophys. Res. Lett.* **32,** L02604, doi:10.1029/2004GL021592 (2005).
32. Knutti, R. & Tomassini, L. Constraints on the transient climate response from observed global temperature and ocean heat uptake. *Geophys. Res. Lett.* **35,** L09701, doi:10.1029/2007GL032904 (2008).
33. Knutti, R., Stocker, T. F., Joos, F. & Plattner, G. K. Probabilistic climate change projections using neural networks. *Clim. Dyn.* **21,** 257–272 (2003).
34. Gregory, J. M., Stouffer, R. J., Raper, S. C. B., Stott, P. A. & Rayner, N. A. An observationally based estimate of the climate sensitivity. *J. Clim.* **15,** 3117–3121 (2002).
35. Forest, C. E., Stone, P. H. & Sokolov, A. P. Estimated PDFs of climate system properties including natural and anthropogenic forcings. *Geophys. Res. Lett.* **33,** L01705, doi:10.1029/2005GL023977 (2006).
36. Andronova, N. G. & Schlesinger, M. E. Objective estimation of the probability density function for climate sensitivity. *J. Geophys. Res.* 106, D19 22605–22611 (2001).
37. Piani, C., Frame, D. J., Stainforth, D. A. & Allen, M. R. Constraints on climate change from a multi-thousand member ensemble of simulations. *Geophys. Res. Lett.* **32,** L23825, doi:10.1029/2005GL024452 (2005).
38. Murphy, J. M. *et al.* Quantification of modelling uncertainties in a large ensemble of climate change simulations. *Nature* **430,** 768–772 (2004).
39. Annan, J. D. & Hargreaves, J. C. Using multiple observationally-based constraints to estimate climate sensitivity. *Geophys. Res. Lett.* **33,** L06704, doi:10.1029/2005GL025259 (2006).
40. Hegerl, G. C., Crowley, T. J., Hyde, W. T. & Frame, D. J. Climate sensitivity constrained by temperature reconstructions over the past seven centuries. *Nature* **440,** 1029–1032 (2006).
41. Knutti, R., Meehl, G. A., Allen, M. R. & Stainforth, D. A. Constraining climate sensitivity from the seasonal cycle in surface temperature. *J. Clim.* **19,** 4224–4233 (2006).
42. Clarke, A. W. & Trinnaman, J. A. (eds) *Survey of Energy Resources 2007* (World Energy Council, 2007).
43. BP. *BP Statistical Review of World Energy June 2008* (BP, London, 2008); available at ⟨www.bp.com/statisticalreview⟩.
44. Rempe, H. Schmidt, S. & Schwarz-Schampera, U. *Reserves, Resources and Availability of Energy Resources 2006* (German Federal Institute for Geosciences and Natural Resources, 2007).
45. Abraham, K. International outlook: world trends: Operators ride the crest of the global wave. *World Oil* 228, no. 9 (2007).
46. Radler, M. Special report: Oil production, reserves increase slightly in 2006. *Oil Gas J.* 104, 20–23 (2006); available at ⟨http://www.ogj.com/currentissue/index.cfm?p=7&v=104&i=47⟩.